Probing Electron-Electron Interaction in Quantum Hall Systems with Scanning Tunneling Spectroscopy

S. Becker,[1] C. Karrasch,[2] T. Mashoff,[1] M. Pratzer,[1] M. Liebmann,[1] V. Meden,[2] and M. Morgenstern[1]

[1]*II. Physikalisches Institut B and JARA-FIT, RWTH Aachen University, 52074 Aachen, Germany*

[2]*Institut für Theorie der Statistischen Physik and JARA-FIT, RWTH Aachen University, 52074 Aachen, Germany*

(Received 7 December 2010; published 13 April 2011)

Using low-temperature scanning tunneling spectroscopy applied to the Cs-induced two-dimensional electron system (2DES) on p-type InSb(110), we probe electron-electron interaction effects in the quantum Hall regime. The 2DES is decoupled from bulk states and exhibits spreading resistance within the insulating quantum Hall phases. In quantitative agreement with calculations we find an exchange enhancement of the spin splitting. Moreover, we observe that both the spatially averaged as well as the local density of states feature a characteristic Coulomb gap at the Fermi level. These results show that electron-electron interaction can be probed down to a resolution below all relevant length scales.

DOI: 10.1103/PhysRevLett.106.156805 PACS numbers: 73.21.Fg, 68.37.Ef, 71.70.Gm, 73.61.Ey

Quantum Hall (QH) physics [1] is a paradigm for the study of interacting quantum systems [2]. In this respect, the III–V semiconductors are very mature materials, although graphene catches up [3]. The most intriguing QH phases are driven by electron-electron (e-e) interaction [4,5], which, however, is screened by nearby gates and competes with disorder. Thus, a central challenge towards a microscopic investigation of QH physics dominated by e-e interaction is to provide a sufficiently clean and electrically decoupled system probed down to the relevant length scales, most notably the magnetic length $l_B = \sqrt{\hbar/(eB)} \simeq$ 10 nm (6 T). Scanning tunneling spectroscopy (STS) achieves the required nm resolution. Applying STS to an adsorbate induced 2D electron system (2DES) [6,7], some of us have shown that the states responsible for the integer QH transitions can indeed be probed with nm resolution [8,9]. Theoretical analysis [10] of these data and similar experimental results for graphite and graphene [11] have also been published.

Here, we modify the 2DES in order to fully decouple it from the substrate and to reduce the disorder. This allows us to probe e-e interaction effects. In particular, we observe an exchange enhancement (EE) of the spin splitting at odd filling factors in quantitative agreement with a parameter-free calculation. Moreover, we measure a Coulomb gap in the spatially averaged density of states (DOS) at the Fermi level E_F. This Coulomb suppression is in quantitative agreement with predictions for localized systems [12–14]. Interestingly, we find a similar suppression in the *local* DOS (LDOS) which is probably caused by fluctuation effects. Observing these hallmarks of the e-e interaction in STS is a crucial step towards a direct imaging of intriguing QH states such as stripe, bubble or fractional QH [4,15] phases.

The home-built scanning tunneling microscope operates at $T = 5$ K in ultrahigh vacuum (UHV) [16]. The dI/dV curves representing the LDOS of the sample are measured by lock-in technique at constant tip-surface distance stabilized at current $I_{\rm stab}$ and voltage $V_{\rm stab}$. A modulation voltage $V_{\rm mod}$ is used to detect dI/dV while ramping the sample voltage V.

The 2DES was prepared in UHV by cleavage of a p-type InSb single crystal ($N_A = 1.1 \times 10^{21}$ m^{-3}) and subsequent Cs adsorption of 1.1% of a monolayer (3.7×10^{16} m^{-2}) onto the cooled (110) surface [17]. The single Cs atoms act as surface donors, which bend the bands downwards and induce a 2DES [6,9,18]. Figure 1(a) shows the corresponding band bending in the near-surface region as calculated by a Poisson solver. This leads to a 2DES with density $N_s \simeq 2.7 \times 10^{16}$ m^{-2}. Note that the band bending reaches deep into the bulk leading to a decoupling of the confined states of the 2DES at E_i, $i \in \mathbb{N}_0$, from the partly empty bulk valence band (BVB) 600 nm apart. Indeed, the spatially averaged dI/dV curve (I) of Fig. 1(b), measured without contacting the 2DES directly, does not exhibit any signature of the 2DES, but only an increase in dI/dV close to the onset of the bulk conduction band (+ 200 mV) and the surface valence band (− 400 mV). The tunneling path from the 2DES to the BVB is blocked. This is in contrast to measurements using n-type [7,9,19] and p-type samples with higher doping [20,21], always exhibiting a step like increase in spatially averaged dI/dV curves close to the calculated E_i. If our 2DES is additionally contacted by an Ag stripe running perpendicular to the cleavage plane [22], it exhibits two steps close to the calculated E_0 and E_1 as visible in curve (II) of Fig. 1(b).

Applying a magnetic field B perpendicular to the 2DES results in peaks corresponding to Landau levels (LLs) and spin levels of the 2DES [curve (III), Fig. 1(b)]. Their distance is in accordance with the effective mass m^* and g factor g^* of the InSb conduction band [17]. The width of the peaks at lower energy is $\Delta E \simeq 16$ meV which is caused by the potential disorder, mainly given by the dopants of the substrate. The Cs atoms, which are ionized by only 30% [23], have a minor effect [7].

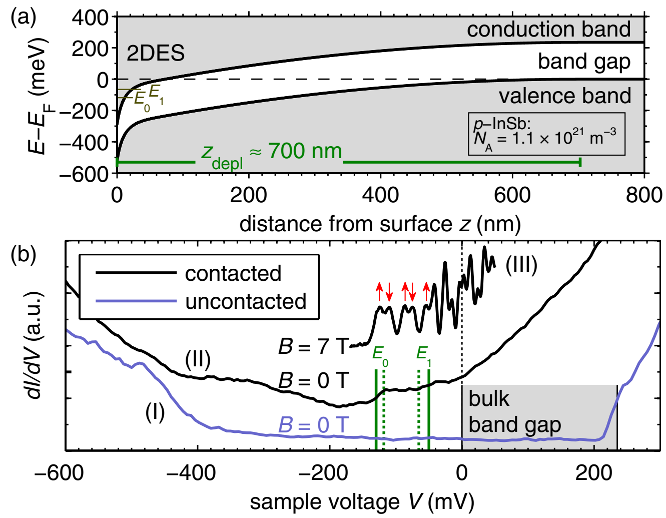

FIG. 1 (color online). (a) Calculated band bending using 1D Poisson equation; first two 2D subband energies $E_0 = -118$ meV, $E_1 = -65$ meV as calculated using the triangular well approximation [17,35] are marked; corresponding electron distribution is shown in [17]. (b) Spatially averaged dI/dV curves across an area A_{Av}: (I): without contacted 2DES, (II), (III): with contacted 2DES at $B = 0$ T, 7 T as marked; gray area: bulk band gap of p-InSb [36]; E_0, E_1: subband energies from experiment (solid) and calculation (broken lines); arrows in (III) mark spin-split LLs. (I) $V_{stab} = 400$ mV, $I_{stab} = 100$ pA, $V_{mod} = 1$ mV$_{rms}$, $A_{Av} = 200 \times 160$ nm^2; (II) $V_{stab} = 300$ mV, $I_{stab} = 50$ pA, $V_{mod} = 3$ mV$_{rms}$, $A_{Av} = 100 \times 100$ nm^2; (III) $V_{stab} = 300$ mV, $I_{stab} = 200$ pA, $V_{mod} = 0.4$ mV$_{rms}$, $A_{Av} = 300 \times 300$ nm^2.

Further evidence for the electrical decoupling of the 2DES from the BVB is presented in Fig. 2, where dI/dV curves at increasing I_{stab} are shown for different B. All curves are measured at the same lateral position. With increasing B, pairs of lines corresponding to spin-split LLs appear. For $B = 0$ T, increasing I_{stab} does not change the dI/dV spectra. At higher B the spectra are spread in V with increasing I_{stab}. At 7 T, the spin splitting of the lowest LL is increased by 13% and the LL distance is increased by 18%. The spreading is symmetric around $V = 0$ mV, i.e., around E_F. It is attributed to the increased localization of electrons with growing B leading to a decrease of 2D conductivity [2]. The spreading cannot be explained by tip induced band bending (Stark effect) [24], which might increase with B due to a reduced screening of the 2DES. Poisson calculations reveal that the spreading at largest tip-surface distance must be much larger than the spreading induced by the change in tip-surface distance in contrast to experiment. Instead, the spreading is quantitatively reproduced by assuming a thermally activated nearest neighbor hopping of the localized electrons within the 2DES from or towards the tip. The model uses barrier heights and next-neighbor distances of valleys as determined from spatially resolved dI/dV data [17] and assumes a reasonable attempt frequency of $\nu_0 = 10^{13}$ Hz [25]. The resulting peak

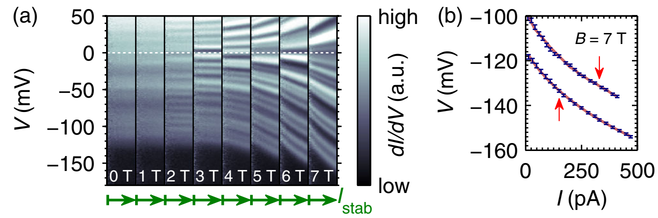

FIG. 2 (color online). (a) dI/dV spectra (gray scale) recorded at the same lateral position at different B fields as indicated. I_{stab} is increased for each B from 100 pA to 2000 pA (left to right). $V_{stab} = 300$ mV, $V_{mod} = 1.6$ mV$_{rms}$. (b) Measured lowest LL positions (spin-up ↑; spin-down ↓) at $B = 7$ T (symbols) in comparison with calculated LL positions (line). Note that the current I at the peak position and not I_{stab} is used as the x axis.

positions in comparison with the experimental data for $B = 7$ T are shown in Fig. 2(b). The excellent agreement strongly supports our assumption that the current indeed flows along the 2DES exhibiting reduced conductivity with increasing B.

The surface 2DES, thus, is occupied, exhibits Landau as well as spin quantization, has moderate disorder, and is decoupled from the bulk electrons of InSb. Moreover, the center of mass of the 2DES is 8 nm below the surface and, thus, sufficiently far from the metallic tip to prevent complete screening. These are the requirements to observe e-e interaction effects within the QH regime. One such effect is the EE of the spin splitting. Loosely speaking the effective repulsion between electrons with parallel spins is smaller than the one for antiparallel spins. This eventually leads to an increase of the spin splitting energy E_{SS} at odd filling factors [26]. Figure 3(a) shows dI/dV spectra taken at a fixed position while ramping the magnetic field B providing the so-called Landau fan. Less than 10% of the fanning is caused by the spreading resistance described above. Varying B, the conductance lines are wavy and deviate from $E^n_{i,\pm} = E_i + \hbar\omega_c(n + \frac{1}{2}) \pm \frac{1}{2} g^* \mu_B B$ with subband index i, LL index $n \in \mathbb{N}_0$, spin index $\pm$, cyclotron frequency $\omega_c = eB/m^*$, and Bohr magneton μ_B. One obvious reason for waviness is a shift of E_F with magnetic field taking place once the increasing degeneracy of a LL favors a transition to the next LL. More importantly, g^* is filling factor dependent due to the EE. To analyze this in more detail, we concentrate on the lowest LL around -120 mV, which gives the highest accuracy in determining E_{SS}. We adapted two Gaussians for all 386 spectra between 3.5 and 6.1 T [27]. The fits are good as can be seen in the inset of Fig. 3(b) and by the confidence value of $R^2 = 0.94$ (0.97 above 5 T). The error for the resulting E_{SS} is about 0.2 meV. $E_{SS}(B)$ is shown in Fig. 3(b) in comparison to a straight line corresponding to ordinary Zeeman splitting of $|g^*|\mu_B B$ with $|g^*| = 42$. Figure 3(c) shows the deviation $\Delta(B)$ from the straight line. It oscillates around 0 meV with maxima (minima) around odd (even) filling factors as expected for EE [28]. The not expected negative values

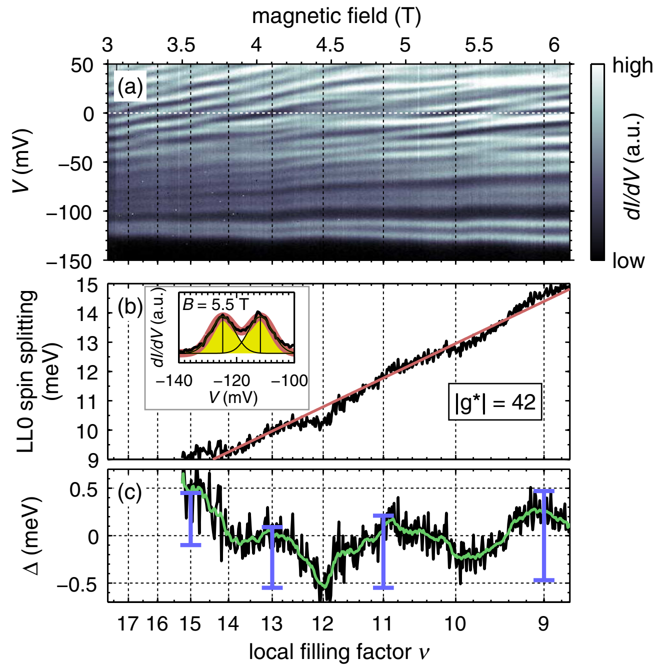

FIG. 3 (color online). (a) Landau fan showing dI/dV as gray-scale; B field ramped downwards, $V_{\mathrm{stab}} = 300$ mV, $I_{\mathrm{stab}} = 400$ pA, $V_{\mathrm{mod}} = 1.6$ $\mathrm{mV_{rms}}$. (b) Spin splitting energy E_{SS} of lowest LL extracted by Gaussian fits as shown in the inset. Straight line marks $E_{\mathrm{SS}} = |g^*|\mu_B B$. (c) Deviation Δ from the linear fit in (b). The inner bright line is smoothed. Vertical bars show the calculated values of EE between neighboring odd and even filling factors. Local filling factors $\nu \propto 1/B$ are matched by counting spin levels below E_F [compare Fig. 4(b)] and verifying their B dependence.

of $\Delta(B)$ are probably caused by slight deviations from a spin splitting linear in B due to either increasing spreading with B, which leads to superlinearity, or nonparabolicity of InSb leading to a smooth decrease of g^*, thus, supralinearity. However, both effects cannot explain oscillations in $\Delta(B)$. One could imagine that spreading depends also on filling factor, but that would lead to an oscillation with maxima at even filling factor.

Moreover, the amplitude of the $\Delta(B)$ oscillation is about 0.7 meV in excellent agreement with theoretical estimates for EE [vertical bars in Fig. 3(c)]. They are obtained by treating the Coulomb interaction using a random phase approximation. This is well justified since the subband electron density N_0 is large compared to the scale set by the Bohr radius [17,26,29]. We performed the calculation using $m^* = 0.02m_0$ and $g^* = -42$ but emphasize that the results barely change if these or other system parameters are varied within reasonable limits (e.g., less than 1% for $g^* = -38$). Thus, magnitude and oscillation phase of $\Delta(B)$ compare favorably with a parameter-free calculation of EE. This implies that the *short-ranged e-e* interaction effect EE can be probed by STS.

For localized electrons interacting via the *long-ranged* part of the Coulomb repulsion, the averaged tunneling DOS is expected to show a gap at E_F [12–14]. For a 2DES with unscreened repulsion at $T = 0$ K, a qualitative analysis gives [13,14]

$$D_0(E) = \frac{2}{\pi}\frac{(4\pi\varepsilon_0\varepsilon_r)^2}{e^4}|E - E_F|. \qquad (1)$$

More elaborate analytical and numerical results leave no doubt about the existence of a Coulomb gap while the exact shape remains controversial [14,30]. This is due to the underlying (spin-)glass physics [30] known to be notoriously complex. A linear Coulomb gap was deduced from various experiments [31]. In our case, where the ratio between disorder and *e-e* interaction is $R = \Delta E/[(e^2\sqrt{N_s})/(4\pi\varepsilon_r\varepsilon_0)] \simeq 1.1$, we also find a dip in the DOS at E_F. Figure 4(a) shows the *spatially averaged* dI/dV curve (thick line) at $B = 7$ T. Instead of a peak at E_F, one observes a double-peak with a minimum at 0 mV. The sum of two identical Gaussian peaks (thin lines)—mimicking the two spin levels of this particular LL (see [17])—matches the measured DOS except of a suppression at E_F. Taking the difference between measured DOS and the sum of the two Gaussians eliminates all single-particle effects leaving only the dip at E_F (medium line). If we modify Eq. (1) to account for finite temperature and screening effects [14] as well as for the energy resolution of our experiment of 1.6 meV [17], we obtain the dotted curve in Fig. 4(a). It shows excellent agreement with the

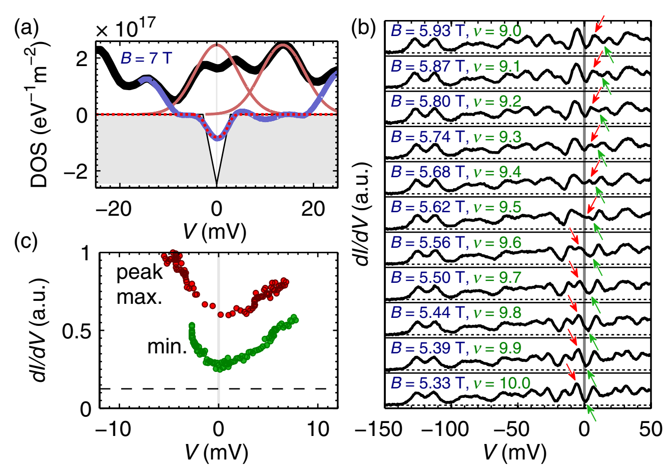

FIG. 4 (color online). (a) Zoom of Fig. 1(b) (III) (thick line), additional Gaussian fits for the LL at E_F (thin lines), and a plot of the difference (medium, blue line) in comparison with the expected bare Coulomb gap of Eq. (1) (V-shaped line) and the Coulomb gap taking finite temperature, screening and energy resolution into account (dotted line); absolute scale of DOS is deduced by fitting the lowest spin-split LL to a two-peak Gaussian and matching the integral of one Gaussian to the known level degeneracy $eB/(2\pi\hbar)$. (b) dI/dV spectra taken at the same position at B as marked. Arrows of same color follow the same peak or minimum across E_F; a movie of the data is available in [17] (c) dI/dV value of the marked peak and minimum in (b) as a function of energy (voltage).

measured dip. The screening is taken to be caused by the STM tip being 8.6 nm away from the center of mass of the 2DES [17]. Note that we observe the gap even around the critical state, i.e., close to half filling of a spin-polarized LL, which is consistent with numerical studies [32]. The facts that we do not observe the dip at E_F without localization (at $B = 0$ T) and that we can reproduce it by a reasonable, parameter-free calculation strongly suggests that we observe the Coulomb gap. We can rule out inelastic excitations as a cause which would lead to much larger half widths of the gap (optical phonons: 22 meV, plasmons: 60 meV, spin excitations: 18 meV) and we are not aware of any many-particle mechanism besides the long-ranged Coulomb repulsion of localized electrons leading to a gap with the observed characteristics.

Surprisingly, a Coulomb gap—although typically thought of being a phenomenon related to disorder averaging or spatial averaging—is also observed in the *local* DOS [33]. The intensity of a particular LDOS peak is suppressed when moved through E_F by increasing B. Figure 4(b) shows corresponding dI/dV curves at fixed position. The upper arrows follow a single spin level as it crosses E_F and the peak intensity is plotted in Fig. 4(c). A minimum intensity is observed exactly at E_F ($B = 5.62$ T) where the peak is suppressed by 48% (suppression in averaged DOS: 33%). The same kind of dI/dV suppression is found for the minimum between LLs, which is marked by the lower lying arrows in (b) and plotted in (c), too. A dI/dV suppression at E_F is also found for fixed B, if different positions are probed within the potential landscape [17]. The finding of Coulomb suppression in the LDOS requires further studies and might be related to Coulomb glass dynamics [34].

In summary, we have shown that low-temperature STS is able to detect e-e interaction in QH samples down to a resolution below all relevant length scales. We have found an exchange enhancement (EE) of the spin splitting at odd fillings and a Coulomb suppression of the averaged as well as of the local DOS at E_F. The EE is in quantitative agreement with a well justified theory, while, due to the less clear status of theory, the comparison for the Coulomb gap is with calculations based on qualitative arguments only. No well-developed theory for the LDOS exists and we conjecture that the Coulomb gap in LDOS is related to (spin-)glass physics.

We acknowledge support by the DFG (MO 858/11-1).

[1] K. v. Klitzing, G. Dorda, and M. Pepper, Phys. Rev. Lett. **45**, 494 (1980).
[2] R. E. Prange *et al.*, *Quantum Hall Effect* (Springer, Berlin, 1986).
[3] X. Du *et al.*, Nature (London) **462**, 192 (2009); K. I. Bolotin *et al.*, Nature (London) **462**, 196 (2009); Y. J. Song *et al.*, Nature (London) **467**, 185 (2010); N. Levy *et al.*, Science **329**, 544 (2010).
[4] D. C. Tsui, H. L. Stormer, and A. C. Gossard, Phys. Rev. Lett. **48**, 1559 (1982); M. P. Lilly *et al.*, Phys. Rev. Lett. **82**, 394 (1999).
[5] S. E. Barrett *et al.*, Phys. Rev. Lett. **74**, 5112 (1995).
[6] V. Y. Aristov *et al.*, Europhys. Lett. **26**, 359 (1994).
[7] M. Morgenstern *et al.*, Phys. Rev. Lett. **89**, 136806 (2002).
[8] M. Morgenstern *et al.*, Phys. Rev. Lett. **90**, 056804 (2003).
[9] K. Hashimoto *et al.*, Phys. Rev. Lett. **101**, 256802 (2008).
[10] T. Champel and S. Florens, Phys. Rev. B **80**, 161311(R) (2009).
[11] D. L. Miller *et al.*, Nature Phys. **6**, 811 (2010); Y. Niimi, H. Kambara, and H. Fukuyama, Phys. Rev. Lett. **102**, 026803 (2009); A. Luican *et al.*, Phys. Rev. B **83**, 041405 (2011).
[12] M. Pollak, Discuss. Faraday Soc. **50**, 13 (1970).
[13] A. L. Efros *et al.*, J. Phys. C **8**, L49 (1975).
[14] F. G. Pikus and A. L. Efros, Phys. Rev. B **51**, 16871 (1995).
[15] J. P. Eisenstein *et al.*, Phys. Rev. Lett. **88**, 076801 (2002).
[16] T. Mashoff *et al.*, Rev. Sci. Instrum. **80**, 053702 (2009).
[17] See supplemental material at http://link.aps.org/supplemental/10.1103/PhysRevLett.106.156805.
[18] M. G. Betti *et al.*, Phys. Rev. B **63**, 155315 (2001).
[19] K. Kanisawa *et al.*, Phys. Rev. Lett. **86**, 3384 (2001).
[20] J. Wiebe *et al.*, Phys. Rev. B **68**, 041402(R) (2003).
[21] S. Becker *et al.*, Phys. Rev. B **81**, 155308 (2010).
[22] R. Masutomi *et al.*, Appl. Phys. Lett. **90**, 202104 (2007).
[23] M. Getzlaff *et al.*, Phys. Rev. B **63**, 205305 (2001).
[24] R. M. Feenstra *et al.*, J. Vac. Sci. Technol. B **5**, 923 (1987); R. Dombrowski *et al.*, Phys. Rev. B **59**, 8043 (1999).
[25] Details will be subject of a forthcoming publication.
[26] T. Ando *et al.*, J. Phys. Soc. Jpn. **37**, 1044 (1974).
[27] Gaussians of equal width and height were fitted using a nonlinear least squares method and a trust-region algorithm as implemented in MATLAB, see MathWorks Curve Fitting Toolbox V2.1 User's Guide.
[28] J. F. Janak, Phys. Rev. **178**, 1416 (1969).
[29] A. P. Smith, A. H. MacDonald, and G. Gumbs, Phys. Rev. B **45**, 8829(R) (1992).
[30] A. Glatz *et al.*, J. Stat. Mech. (2008) P06006.
[31] V. Y. Butko, J. F. DiTusa, and P. W. Adams, Phys. Rev. Lett. **84**, 1543 (2000); R. C. Ashoori *et al.*, Phys. Rev. B **48**, 4616 (1993); H. B. Chan *et al.*, Phys. Rev. Lett. **79**, 2867 (1997); E. V. Deviatov *et al.*, Phys. Rev. B **61**, 2939 (2000).
[32] S.-R. E. Yang and A. H. MacDonald, Phys. Rev. Lett. **70**, 4110 (1993).
[33] M. Morgenstern *et al.*, Phys. Rev. B **66**, 121102(R) (2002).
[34] D. Menashe *et al.*, Phys. Rev. B **64**, 115209 (2001).
[35] T. Ando, J. Phys. Soc. Jpn. **53**, 3101 (1984).
[36] I. Vurgaftman *et al.*, J. Appl. Phys. **89**, 5815 (2001).